PLOS ONE

RESEARCH ARTICLE

Adaptations of an RNA virus to increasing thermal stress

Sonia Singhal¤*, Cierra M. Leon Guerrero, Stella G. Whang, Erin M. McClure, Hannah G. Busch, Benjamin Kerr

Department of Biology, University of Washington, Seattle, WA, United States of America

¤ Current address: Department of Biology, University of North Carolina, Chapel Hill, NC, United States of America
* ssinghal@email.unc.edu

Citation: Singhal S, Leon Guerrero CM, Whang SG, McClure EM, Busch HG, Kerr B (2017) Adaptations of an RNA virus to increasing thermal stress. PLoS ONE 12(12): e0189602. https://doi.org/10.1371/journal.pone.0189602

Editor: Suzannah Rutherford, Fred Hutchinson Cancer Research Center, UNITED STATES

Received: July 13, 2017

Accepted: November 28, 2017

Published: December 21, 2017

Data Availability Statement: All data files and analysis scripts used in this study are available from figshare at https://doi.org/10.6084/m9.figshare.5591227. The nucleotide sequence of the ancestral virus used in this study is available from GenBank, accession # MF352213-MF352215.

Funding: This work was supported by the following grants: the National Science Foundation (NSF; https://www.nsf.gov/) under Cooperative Agreement DBI-0939454 (to BK); an NSF CAREER Award to BK (Grant DEB0952825); an NSF Graduate Research Fellowship to SS (Awards DGE-

Abstract

Environments can change in incremental fashions, where a shift from one state to another occurs over multiple organismal generations. The *rate* of the environmental change is expected to influence how and how well populations adapt to the final environmental state. We used a model system, the lytic RNA bacteriophage Φ6, to investigate this question empirically. We evolved viruses for thermostability by exposing them to heat shocks that increased to a maximum temperature at different rates. We observed increases in the ability of many heat-shocked populations to survive high temperature heat shocks. On their first exposure to the highest temperature, populations that experienced a gradual increase in temperature had higher average survival than populations that experienced a rapid temperature increase. However, at the end of the experiment, neither the survival of populations at the highest temperature nor the number of mutations per population varied significantly according to the rate of thermal change. We also evaluated mutations from the endpoint populations for their effects on viral thermostability and growth. As expected, some mutations did increase viral thermostability. However, other mutations *decreased* thermostability but increased growth rate, suggesting that benefits of an increased replication rate may have sometimes outweighed the benefits of enhanced thermostability. Our study highlights the importance of considering the effects of multiple selective pressures, even in environments where a single factor changes.

Introduction

The process of *de novo* adaptation is typically studied in the context of the simplest form of environmental change, an abrupt shift from one environmental state to another (e.g., [1]). A population is typically poorly adapted to the new environmental state, so this shift reduces its mean fitness. Mean fitness then increases as the population gains and fixes beneficial mutations. For instance, under Fisher's geometric model [2], the population is expected first to fix mutations that confer large gains in fitness, followed by mutations of increasingly smaller benefit as the population approaches the optimal phenotype in the new environment [1].

However, natural environments rarely change in the simple, abrupt fashion assumed by such models. Rather, environmental changes can occur more gradually, on scales that

0718124 and DGE-1256082); a Ronald E. McNair Post-Baccalaureate Scholarship to CMLG (http://depts.washington.edu/uwmcnair/); a Mary Gates Research Scholarship to EMM (http://expd.uw.edu/mge/about/); and a Walter and Margaret Sargent Award (to EMM) and Kathryn C. Hahn Writing Fellowship (to SS) from the University of Washington Department of Biology (https://www.biology.washington.edu/about-us/support-uw-biology). The funders had no role in study design, data collection and analysis, decision to publish, or preparation of the manuscript.

Competing interests: The authors have declared that no competing interests exist.

encompass multiple organismal generations. For example, shifts between glacial and interglacial periods occurred over thousands of years (e.g., [3]). Even changes that are rapid on geological scales, such as anthropogenic climate change (e.g., [4]) or changes in pollution levels (e.g., [5]), occur over multiple decades. Adaptation may proceed very differently in such cases of incremental environmental change [6–8].

Evolution in an incrementally changing environment is often modeled as a single quantitative trait evolving under Gaussian stabilizing selection in conditions where the optimal phenotype is constantly shifting [6, 8–13]. In contrast to adaptation under rapid environmental change, adaptation under gradual change is more likely to proceed via fixation of mutations that provide small shifts in phenotype and thus small increases in fitness [6–8]. These shifts allow an evolving population to track the optimal phenotype, but with a lag. The larger the phenotypic lag, the lower the mean fitness of the evolving population. The rate of environmental change can influence the adaptive process by setting the rate at which the population must track changes in the optimal phenotype. More rapid changes in the optimal phenotype typically result in a larger lag of the quantitative trait [6, 8, 11, 12, 14–16]. If a larger distance between the population's mean phenotype and the optimal phenotype also results in the death of a larger number of individuals, then sufficiently rapid environmental change can lead to population collapse due to consequent loss of genetic variation [11–13, 17, 18].

The assumptions made by theoretical models may not always be met in biological systems. For this reason, empirical studies using microorganisms have been important in refining our understanding of evolution in incrementally changing environments. In some studies, and in line with model predictions, the rate of population extinction is lower under more gradual environmental change [19–21]. While models predict a higher mean fitness under gradual than rapid environmental change (due to a smaller lag between the population's mean phenotype and the optimal phenotype), these models tend to consider unlimited change. In contrast, many experiments set limits on the maximum amount of change in the environment. In this framework, the level of environmental stress increases to a maximal level at different rates, and treatments involving more rapid change reach the maximum sooner and remain there longer. Such studies yield heterogeneous results of adaptation at the environmental limit. Exposure to low levels of stress can sometimes increase the probability that a population will survive at the environmental limit [20–23]. In some studies, adaptive phenotypes obtained under gradual environmental change have higher fitness in the most stressful environment than phenotypes obtained under rapid environmental change [7, 24, 25]. In other studies, adaptive phenotypes obtained under rapid environmental change are fitter [19, 20, 23]. One study found that the rate of environmental change did not affect fitness in the ultimate environment [26].

Empirical studies have also revealed complexities in how the rate of environmental change affects the amount of genetic variation present during the adaptive process. Higher population sizes and less extreme selection coefficients under more gradual environmental change may permit greater genetic diversity [21, 24]. In asexual microbial populations, clonal interference, where distinct beneficial mutations arise in different genetic backgrounds that cannot recombine [27], may also have a greater effect under gradual environmental change if multiple mutations of small effect are available simultaneously [24, 25, 28]. On the other hand, when environmental change cannot exceed a maximal value, populations under gradual change must survive in both intermediate and extreme environments, while populations experiencing the most rapid change must only survive the most extreme environment. If the exposure to a greater diversity of selective environments constrains mutations beneficial in all environments, then a greater diversity of mutations would be predicted under rapid change [7]. Consistent with this hypothesis, some studies find greater variability in phenotypes [7, 19] or fixed mutations [25] under rapid than attenuated environmental change.

Given the heterogeneous results from prior experiments, further experimental studies with different organisms and environmental factors are warranted. In this study, we exposed populations of the lytic RNA bacteriophage Φ6 to heat shocks that increased to a high temperature maximum at varying rates. Subjecting the viruses (but not the host) to heat stress promotes the evolution of thermotolerance via greater stability of viral proteins: Only viruses that survive heat stress with little enough damage that they can subsequently infect a host cell are able to replicate. To track adaptation over time, we measured the percent of the viral population that was able to survive heat shock at each transfer.

We aimed to address how varying rates of thermal change would affect viral evolution in:

1. **Survival on the first exposure to the most extreme environment**. Assuming that mutations that enable survival at intermediate temperatures also contribute to survival at the highest temperature, we predicted that populations under gradual thermal change would have a greater survival when they first reached the highest temperature because they had more time to gain and fix thermostabilizing mutations.
2. **Survival in the most extreme environment at the end of the experiment**. On the one hand, populations that experienced the most rapid change in temperature would also have more time to adapt under the highest temperature, favoring higher final fitness in this treatment. On the other hand, if mutations selected under intermediate temperatures serve as genetic backgrounds for additional mutations that confer high fitness under high temperatures, then populations that experienced a more gradual change in temperature might have higher survival in the ultimate environment (see [21] for a discussion of such epistatic effects in the context of adaptation in changing environments).
3. **The quantity and effect sizes of mutations that permit survival at high temperatures**. We predicted that thermostability would increase more often through single mutations of large effect in environments that changed rapidly, while thermostability would be more likely to increase through multiple mutations of small effect in environments that changed more gradually.

While we did find that evolution at intermediate temperatures enhanced the ability of populations to survive their first exposure to the highest temperature, similar adaptive endpoints were accessible under all rates of environmental change, and the ultimate survival at the highest temperature did not differ across treatments. We also found no strong relationship between the rate of environmental change and the number or effect size of mutations. In addition, we found that selective pressures orthogonal to those of the changing environment can still play a major role in shaping adaptive solutions in stressful environments.

Methods

Strains and culture conditions

A list of all viral and bacterial strains used or engineered in this study appears in S1 Table.

Φ6 Cystovirus has a tripartite genome made of double-stranded RNA. The particular strain used in this study originated from three plasmids containing cDNAs of each of the wild type Φ6 segments [29, 30]. These plasmids were co-transformed into bacterial host cells (*Pseudomonas syringae* pathovar *phaseolicola*) to make phage particles [29, 30] (see section on Reverse engineering, below, for details). L. Mindich (Rutgers University, Newark, New Jersey) kindly provided the following strains: LM4286 (contains pLM687 with the Φ6 L segment [31]), LM4284 (contains pLM656 with the Φ6 M segment [32]), LM4285 (contains pLM659 with the

Φ6 S segment [33, 34]), and LM987 (contains pLM857 with the Φ6 M segment and a *lacH* marker, which creates phages that make blue plaques [35]).

The laboratory bacterial host for Φ6 growth, *P. phaseolicola* HB10Y, derives from ATCC #21781. Transformation of the phage plasmids was performed into LM2691, a variant of *P. phaseolicola* HB10Y containing a plasmid with a T7 reverse transcriptase [36, 37] (see also section on Reverse engineering). Both of these hosts were kindly supplied to our laboratory by C. Burch (University of North Carolina, Chapel Hill). During competition assays, counts of clear and blue Φ6 plaques (made from plasmid pLM857) were distinguished on bacterial lawns of a second HB10Y variant, LM1034 (kindly provided by L. Mindich), which contained a plasmid with a lac omega gene [35].

Host cultures were initialized from individual colonies and grown overnight at 25˚C in LC medium (Luria-Bertani broth at pH 7.5). Antibiotics (15 μg/mL tetracycline or 200 μg/mL ampicillin) were added to cultures of LM2961 or LM1034, respectively, to maintain their plasmids.

Each viral lysate was prepared from a plaque that had been isolated and stocked in 500 μL of 4:6 (v/v) glycerol:LC. A diluted sample of the virus stock was mixed with 200 μL of stationary-phase of *P. phaseolicola* in LC 0.7% top agar. The mixture was overlaid on an LC 1.5% agar base, and the agar plate was incubated overnight at 25˚C. Plaques were collected and filtered in 3 mL of LC medium through cellulose acetate filters (0.2 μm pore, Thermo Scientific) to remove bacterial cells.

Evolution experiment

A schematic of the evolution experiment is shown in Fig 1.

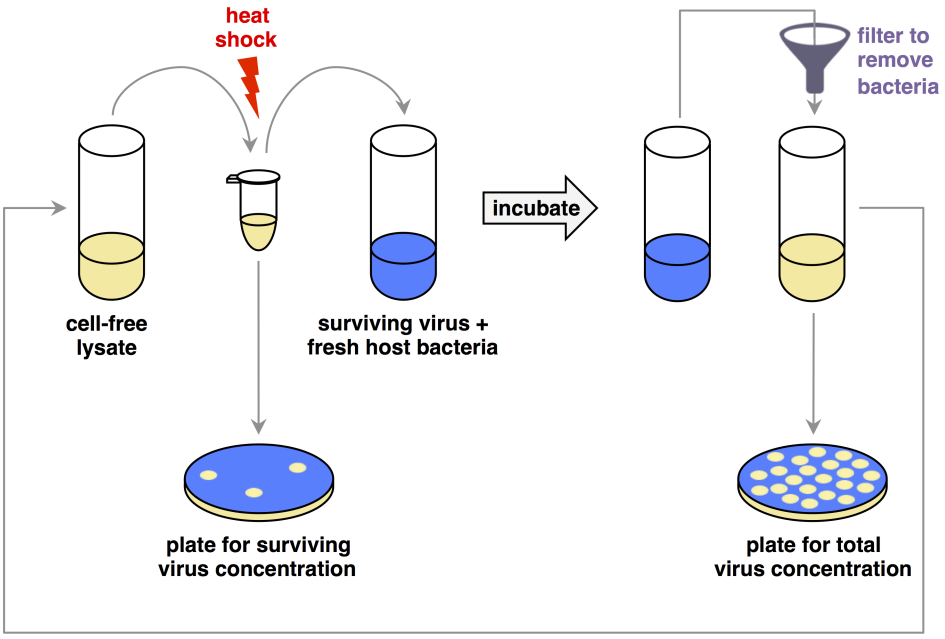

Fig 1. Schematic of the evolution experiment. Bacteria-free lysates of virus were heat shocked for 5 minutes at a pre-specified temperature (Fig 2), then added to culture with naïve host bacteria and grown overnight at 25˚C. After the growth period, the viruses were separated from the bacteria by filtration, and the new cell-free lysate was again heat shocked. In order to track changes in survival to thermal stress, viral lysates were plated for concentration before and after heat shock by mixing a dilution of the lysate with abundant host bacteria in soft agar and spreading it onto a Petri dish. After overnight incubation, we counted plaques in the bacterial lawn, each of which originated from a single viral particle. The experiment ran for 32 transfers (approximately 100 viral generations).

https://doi.org/10.1371/journal.pone.0189602.g001

The evolution experiment was initialized with a lysate made from a single plaque that had resulted from the transformation from plasmids pLM687, pLM656, and pLM659 (see also section on Reverse engineering), prepared as described under the section on Strains and culture conditions. This lysate was divided among 20 populations across four treatments with five replicates each (5 Gradual populations, 5 Moderate populations, 5 Sudden populations, 5 Control populations). Cell-free lysates of each population were heat-shocked at a pre-determined temperature (see section on Calculation of heat shock regimes, below), then added to culture with naïve *P. phaseolicola* for overnight growth at 25˚C. We performed heat shocks on lysates (i.e., without the bacterial host) so that viral evolution was not affected by host heat shock responses. (We had additionally determined that the bacterial host does not survive temperatures above 45˚C.)

Our thermal regimes (Fig 2) paralleled the design used in other studies [7, 21, 25]:

1. **Sudden:** First and all subsequent heat shocks were performed at 50˚C.
2. **Moderate:** Heat shock temperatures increased from 45˚C over the course of evolution, reached 50˚C halfway through the experiment, and remained at that temperature thereafter.
3. **Gradual:** Heat shock temperatures increased from 45˚C and only reached 50˚C on the final transfer.
4. **Control:** Viruses only received a mock "heat shock" at their normal growth temperature (25˚C).

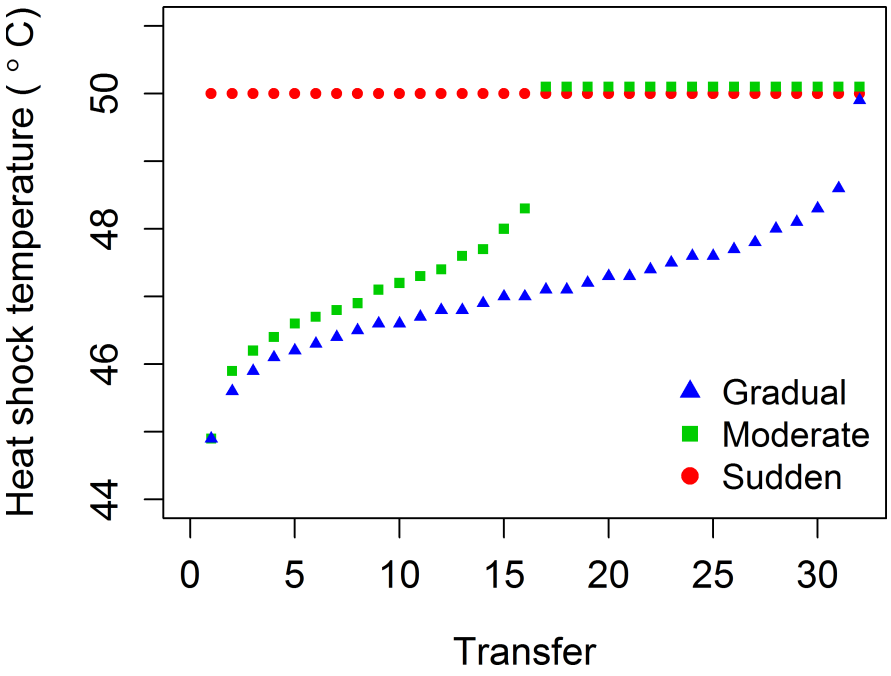

Fig 2. Temperature regimes for experimental evolution with varying rates of thermal change. Points are offset vertically at 50˚C for purposes of visualization. Temperature increments were chosen such that the ancestral virus would experience constant (i.e., linear) decreases in its probability of survival. A control regime of heat shocks at a constant 25˚C (not shown) accounted for evolutionary change under transfer conditions. See also S2 Table.

https://doi.org/10.1371/journal.pone.0189602.g002

Calculation of heat shock treatments

The exact rates of temperature increase were determined empirically from experiments that measured survival of the ancestral genotype between 45–50˚C. A cell-free lysate was prepared as described under the section on Strains and culture conditions and titered on *P. phaseolicola* for pre-heat shock concentrations. The lysate was aliquoted into replicates of 50 μL, and replicates were heat shocked for 5 minutes in a pre-heated thermocyler (BioRad, C1000 Thermal Cycler), then chilled on ice. Heat shocks covered a range of temperatures from 25–54˚C. After heat shock, the replicates were diluted and plated for their post-heat shock concentration. Survival was calculated as the ratio of post- to pre-heat shock titer multiplied by 100. We estimated thermostability across the temperature range using an inverse Hill equation:

$$S = a \times \frac{{T_{50}}^n}{{T_{50}}^n + T^n} \quad (1)$$

where S is the percent survival, a is the survival at the normal growth temperature (25˚C), T is the heat shock temperature, T_{50} is the temperature with 50% viability, and n is the Hill coefficient. Parameters a, T_{50}, and n were estimated using nonlinear least squares minimization.

Thermostability data taken on three separate days were combined to create an ancestral thermal kill curve. Because survival at 25˚C (the laboratory growth temperature for Φ6) varied across days, we first fit Eq 1 to each day separately, and then divided all survivals from that day by its asymptote a so that survival at 25˚C was 100%. The transformed data from all three days were then combined, and Eq 1 re-fit to these data (Fig 3). This ancestral thermal kill curve was used to calculate temperature regimes for the Gradual and Moderate treatments (Fig 2). Increases in temperature in these treatments represented equal reductions in percent survival for the ancestor. Setting these expected percent survivals as S, we calculated the corresponding temperatures by solving Eq 1 for T, using the nonlinear least squares estimations for the values of a, n, and T_{50}. The resulting temperatures were rounded to a single decimal place for use in

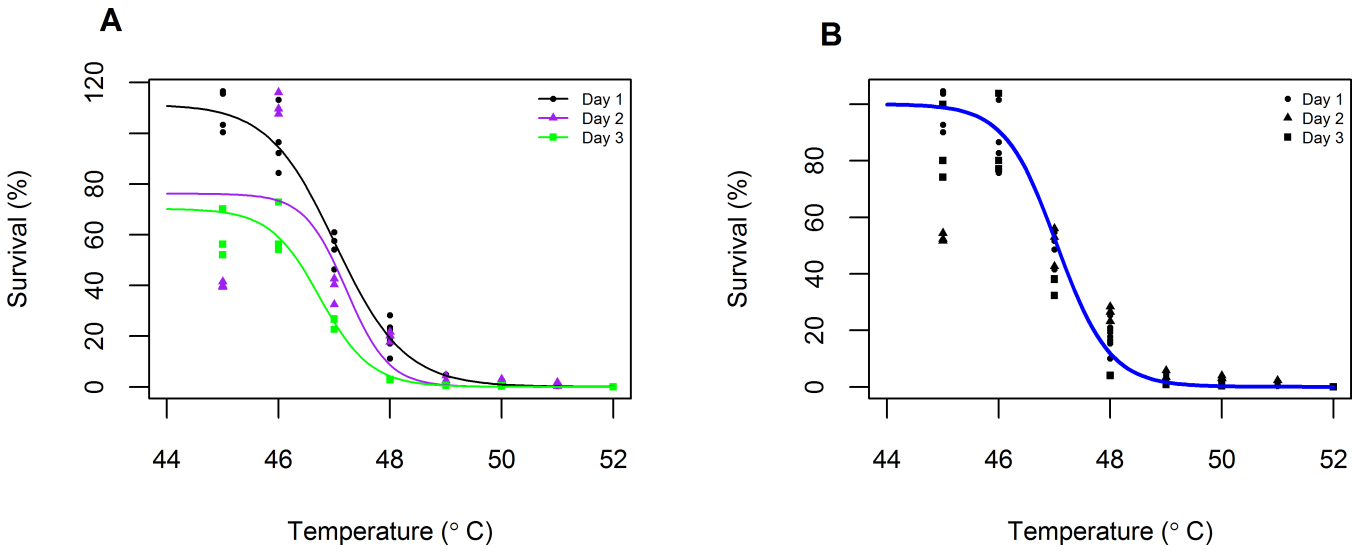

Fig 3. Estimation of the thermal kill curve of the ancestral Φ6 genotype. Temperatures from 44–52˚C are shown to visualize the drop in viral survival. A) On three separate days, a cell-free lysate was exposed to a 5-minute heat shock at each temperature and plated before and afterward to calculate percent survival (points). (Note that, because of stochasticity in determining phage titers, survivals occasionally exceed 100%.) Eq 1 was fitted to the data in R, where the parameters a, T_{50}, and n were estimated by nonlinear least squares (lines). B) Data from each day were then divided by their respective asymptotes a (points). The adjusted data were pooled and Eq 1 re-fit to calculate the ancestral thermal kill curve (line). This curve was used for calculation of the thermal regimes and to set null expectations of viral survival during the evolution experiment.

https://doi.org/10.1371/journal.pone.0189602.g003

the thermocycler (Fig 2, S2 Table). (Further details on calculation of treatment heat shock temperatures are available in the Data Repository.)

Preparation for heat shock

Lysates were created from overnight liquid cultures by centrifuging 800 μL of culture at 10,000 rcf through a cellulose acetate spin filter with a 0.2 μm pore (Costar). The lysate's titer was taken as the mean of duplicate titers on *P. phaseolicola* in agar plates. To control for any density-dependent effects of heat shock on viral survival, we adjusted all lysates by dilution to match the lysate with the lowest titer for that transfer (between 8×10^9 and 2×10^{10} plaque-forming units [pfu] /mL). We note that, across treatments, lysate titers fell within less than an order of magnitude of each other, and the treatment to which lowest-titer lysate belonged varied across transfers.

The titer-adjusted lysates were diluted and plated on *P. phaseolicola* for their pre-heat shock concentrations.

Heat shock

Heat shocks were then performed on the lysates that had been diluted to the same titer. 50 μL of lysate were aliquoted into PCR strip tubes (one tube per replicate population), placed for 5 minutes on a thermocycler (BioRad, C1000 Thermal Cycler) pre-heated to the appropriate temperature (S2 Table), and then chilled on ice. The heat-shocked lysates were diluted and plated for post-heat shock concentrations.

Culturing of surviving phages

Viruses that had survived heat shock were introduced to bacterial host cells in liquid culture for amplification. Four mL of LC broth were inoculated with a 1/100 dilution of naïve, stationary-phase *P. phaseolicola* and heat-shocked lysate to a final concentration of approximately 2.5×10^3 viral particles/mL. (These concentrations were approximated based on survivals from the previous transfer, because the exact lysate titers were not known until following day.) We inoculated the viruses at the same concentration across treatments to ensure equal mutational opportunities. Cultures were incubated for 24 hours at 25˚C with orbital shaking to allow the phages to amplify. The cultures were then prepared for the next round of heat shock as described above.

Storage

After each transfer, at least 500 μL of each post-amplification population were mixed with glycerol to a final concentration of 40% and stored long-term at -20˚C.

Reverse engineering

All mutations discussed in this paper were constructed on pLM659, the plasmid containing a cDNA copy of the S segment of ϕ6. Mutations were engineered into this plasmid using the QuikChange II Mutagenesis kit (Agilent) following the manufacturers' instructions. Primers for each mutation are included in S4 Table. Mutagenized plasmids were stored in *Escherichia coli* XL1-Blue bacteria (included in the QuikChange II Mutagenesis kit), and the mutations of interest were confirmed by Sanger sequencing.

Mutation V109I was engineered using mutagenic PCR and T4 ligation. The plasmid pLM659 was PCR amplified from adjacent, overlapping primers with 5' phosphorylated ends, one of which contained the mutation of interest, using Phusion polymerase (Thermo

Scientific) according to the manufacturer's instructions. To remove (unmutagenized) template plasmid, the PCR product was digested with DpnI (New England Biolabs) according to the manufacturer's instructions. Approximately 14 ng of DpnI-digested PCR product were used in a T4 ligation (New England Biolabs) according to the manufacturer's instructions, and the ligation product was transformed into electrocompetent *E. coli* DH5α, prepared as described for LM2691 below, for storage.

Creating phage particles involved transforming plasmids with each of the Φ6 genomic segments into the bacterium LM2691. We made this strain electrocompetent with the following protocol: A culture of LM2691 was grown to stationary phase, then diluted 1/10 into 50 mL of fresh media and grown to exponential phase. The cells were chilled on ice, then pelleted by centrifugation (6 minutes at 2850 rcf) and washed multiple times with the following resuspensions:

1. 50 mL of ice-cold, sterile water.
2. 15 mL of ice-cold, sterile water.
3. 2 mL of ice-cold 10% glycerol.
4. $<$ 1 mL of ice-cold 20% glycerol (exact volume depended on the number of transformations being performed at the time).

The final suspension of cells was aliquoted into 40-μL volumes for working use.

At least 5 ng of a plasmid containing each Φ6 segment (S, M, and L) were combined with the competent cells (in some cases as much as 100 ng of each plasmid were necessary), incubated on ice for 1 minute, and electroporated on an Eppendorf Eporator in an ice-cold cuvette with a 1-mm gap. The cells were resuspended in 700 μL of SOC medium [38], added to 3 mL of LC 0.7% top agar, plated on LC 1.5% agar plates, and incubated overnight at 25˚C. Successful transformations were indicated by viral plaques in the bacterial lawn. At least 6 plaques per genotype were stored for sequence confirmation (see Sequencing viral genotypes).

The ancestral genotype for the evolution experiment resulted from transformation of the original plasmids, pLM687, pLM656, and pLM659. For engineered phage, an engineered version of pLM659 was combined with the original versions of pLM687 and pLM656. A version of Φ6 marked with *lacH* (used for assaying viral fitness) resulted from transformation of plasmids pLM687, pLM659, and pLM857.

Sequencing viral genotypes

Sequencing was performed on viral lysates from either the stored populations from the evolution experiment or the stored reverse engineered plaques. Lysates were made as described in the section on Strains and culture conditions. RNA was extracted from the lysates using the QIAamp Viral RNA Mini Kit (Qiagen) and reverse transcribed into cDNA using SuperScript II reverse transcriptase (Invitrogen), following the manufacturers' protocols. cDNA samples were PCR amplified with phage-specific primers using touchdown cycling (annealing temperature 65–55˚C for 10 cycles, reducing the temperature by 1˚C each cycle, followed by 25 cycles with a 55˚C annealing temperature). The resulting products were given an ExoSap-IT cleanup (Affymetrix) and Sanger sequenced through GeneWiz. Primers were designed to permit 2x coverage of at least 90% of the genome (excluded sections at the segment ends).

Sequence alignments were performed in Geneious v. 10.0.6 and inspected by eye. The ancestral sequence (GenBank Accession # MF352213-MF352215) was built through alignment against sequence files of the plasmids containing the wild type Φ6 segments (provided by L. Mindich). All other sequences were aligned against the ancestral sequence.

Assaying viral thermostability

We assessed viral thermostability by exposing lysates to heat shocks across a range of temperatures and measuring the change in viral concentration under each temperature.

Cell-free lysates of each evaluated genotype were prepared as described under Strains and culture conditions and titered on *P. phaseolicola*. In individual heat shock assays, we measured 3–5 unique genotypes (plaques) and the ancestral genotype. To control for any concentration-dependent effects of heat shock on viral survival, all lysates were diluted to a target titer of 2.17 x 10^8 viral particles/mL (concentration of the lowest-titer lysate across assay days). The diluted lysates were plated on *P. phaseolicola* for pre-heat shock titers (actual titers fell between 1.0 x 10^8 and 4.8 x 10^8 pfu/mL) and were used for heat shocks.

Lysates were heat shocked over a range of temperatures from 25–54˚C. For each temperature tested, three replicate samples containing 50 μL of lysate were heat-shocked for 5 minutes in a pre-heated thermocycler (BioRad, C1000 Thermal Cycler), then chilled on ice. After heat shock, the lysates were diluted and plated for their survival. Survival of the lysates was calculated as the ratio of post- to pre-heat shock titer multiplied by 100. We estimated viral thermostability across the temperature range using the inverse Hill equation (Eq 1). Genotypes with a greater T_{50} than the ancestor were considered to be more thermostable.

Because the ancestral genotype was assayed alongside each set of engineered mutants, we gained additional data on the ancestor's thermal kill curve. Based on these additional data, we altered certain aspects of parameter estimation. First, we estimated parameters T_{50} and n using maximum log likelihood. This method allowed us to determine whether mutants' thermal kill curves were significantly different from the ancestor's through a likelihood ratio test on two nested models, one that estimated parameters when survivals for the ancestor and focal mutant were pooled, and the other that estimated separate parameters for each lysate. Second, we removed data collected at 25˚C from analysis, since measured survivals were often much greater than 100% (S1 Fig), most likely due to stochasticity in plating assays. Third, because mutants were compared to an ancestral lysate that had been measured concurrently, we did not adjust survivals by their asymptote. (We also found that thermal kill curves of the ancestral genotype taken on different days had T_{50} values that were more similar without adjustment, suggesting that asymptote adjustment did not necessarily reduce inter-day variability for this dataset; see S2 Fig) Finally, to simplify comparisons across thermal kill curves, parameter a was not estimated, but fixed at 100. Full details of these analyses are included in the Data Repository.

Assaying viral competitive fitness

Viral growth rates were evaluated through growth competitions against a marked common competitor, the *lacH*-marked Φ6, under conditions that replicated those of growth during the evolution experiment. Plaques formed by the *lacH*-marked Φ6 turn blue when plated with X-Gal on LM1034 (a bacterial host containing a plasmid with the complementary *lacω* gene), allowing us to distinguish the common competitor from the genotypes engineered for this study.

The common competitor was transformed from the plasmids described above (see section on Reverse engineering). To pre-adapt this strain to the competition conditions, the plaque isolated from the transformation was passaged for five days in LC broth. However, its growth rate remained low compared to the ancestor of the evolution experiment, so competitions were initialized at a 1:10 ratio of focal strain: common competitor. We confirmed that changing the ancestor's initial ratio in the competition did not affect the measured competitive fitness (S3 Fig).

Lysates of the ancestral virus, each mutant virus, and the *lacH*-marked common competitor were made from frozen stocks containing plaques, as described in the section on Strains and culture conditions. Lysates of the focal strains were diluted to a target concentration of 2.89 x 10^8 viral particles/mL, while the lysate of the common competitor was diluted to a target concentration ten times higher (2.89 x 10^9 viral particles/mL). Each diluted focal strain was mixed with an equal volume of the diluted common competitor to create the competition mixture. To obtain initial concentrations of each strain in the competition, the competition mixtures were plated on LM1034 with 100 μL of 40 mg/mL X-Gal (dissolved in DMSO). (Actual concentrations of the focal strains fell between 7.7 x 10^7 and 2.1 x 10^8 pfu/mL, and actual concentrations of the common competitor fell between 6.0 x 10^8 and 2.4 x 10^9 pfu/mL. Actual ratios of focal strain: common competitor ranged between 0.06 and 0.23.)

Cultures were then initialized from the competition mixtures on the normal *P. phaseolicola* host. Competitions were carried out in 4 mL of LC broth with a 1/100 dilution of naïve, stationary-phase *P. phaseolicola*. The competition mixture was added into this culture to a final concentration of approximately 2.5 x 10^3 viral particles/mL (the inoculated concentration used in the evolution experiment; see section on Culturing of surviving phages, under Evolution experiment). Cultures were incubated for 24 hours at 25˚C with orbital shaking.

Final concentrations of each strain were determined by diluting aliquots of the cultures and plating them on LM1034 with 100 μL of 40 mg/mL X-Gal. The competitive fitness of each focal strain was calculated as its change in relative density in the competition over time:

$$W_{1,2} = \frac{C_{f,1}/C_{f,2}}{C_{i,1}/C_{i,2}} \quad (2)$$

where $W_{1,2}$ denotes the calculated competitive fitness of the focal strain, C_i is the initial concentration, C_f is the final concentration, a subscript 1 denotes the focal strain, and a subscript 2 denotes the common competitor. Relative competitive fitness with respect to the ancestral genotype was then calculated by dividing the competitive fitness of each focal genotype by the mean competitive fitness of the ancestor.

Results

Changes in survival to heat shock over time

Viral survival is expected to decrease as the heat shock temperature increases past 45˚C (see Fig 3). Fig 4 compares the observed percent survival of populations in the Gradual, Moderate, Sudden, and Control treatments at each transfer to the expected percent survival of the ancestral genotype at the heat shock temperature experienced in that transfer, calculated from prior thermal kill curves on the ancestral genotype (Fig 3B). If heat-shocked populations did not evolve greater thermostability than the ancestor, then we would expect no average difference between the survival of the population and the ancestor at each temperature (i.e., the point would fall at 0).

We did not find an improvement over time in the survival of the Control population in response to mock heat shocks at 25˚C. (Reductions in survival of the Control population are most likely due to stochasticity introduced when pipetting and plating lysates whose titers differ by less than an order of magnitude.) In contrast, the percent survival of Φ6 from Gradual, Moderate, and Sudden populations was greater than ancestral values for every transfer in the second half of the experiment (Fig 4). Treatments differed in survival to their respective first exposures to 50˚C (analysis of variance, $F(2,12) = 4.83$, $p = 0.03$; Fig 5); specifically, populations from the Gradual treatment had a higher survival than populations from the Sudden treatment on their first exposure to 50˚C (Tukey's post-hoc test, $p = 0.03$; other comparisons

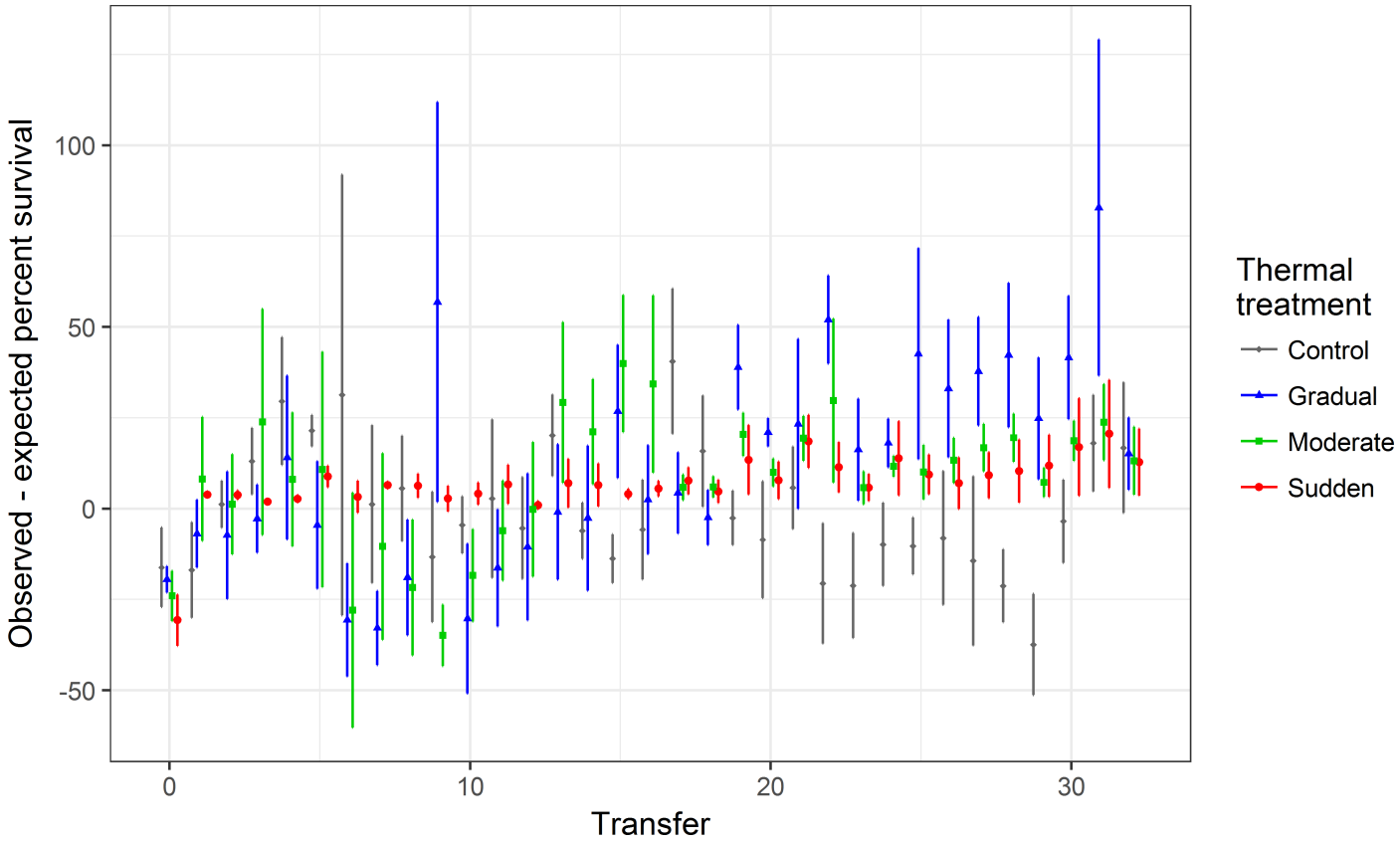

Fig 4. Changes in percent survival of viral lysates to heat shock over time. The survival of each population (Observed percent survival) at each transfer is compared to the percent survival of the ancestor (Expected percent survival) at the temperature used for heat shock (see Fig 2, S2 Table), calculated from the estimated thermal kill curve for the ancestor (Fig 3B). Points represent the average difference between the measured population survival and the calculated ancestral survival; error bars represent the standard deviation of this difference. Treatments in which populations evolved higher thermostability than the ancestor have a difference greater than 0. Note that, because of stochasticity in determining close phage titers, differences occasionally deviate from 0 for treatments that received low-temperature heat shocks. Points are offset horizontally for better visualization.

https://doi.org/10.1371/journal.pone.0189602.g004

were not significant). The survival data thus suggest that heat shocked populations evolved greater thermostability, even during exposure to intermediate temperatures. However, at the end of the experiment, the average survival of Gradual and Moderate populations at 50˚C did not differ significantly from survival of populations from the Sudden treatment (analysis of variance, $F(2, 12) = 0.0872$, $p = 0.92$; Fig 6).

Genetic basis of thermostability

To identify mutations that may have contributed to increases in thermostability, we sequenced the endpoint populations in gene 5 (encodes the P5 lysis protein) and gene 8 (encodes the P8 outer shell protein). As proteins on the exterior of the virus that are necessary for viral infection [39, 40], both P5 and P8 are expected to experience strong selection for thermostability at high temperatures to maintain their functions.

We found a total of 16 distinct mutations across all populations (Table 1), 11 of which were unique to populations that had experienced high-temperature heat shocks. Populations from Gradual and Moderate treatments appeared to have more unique mutations and a larger average number of mutations per lineage than populations from Control and Sudden treatments (Table 2). However, the number of mutations per population did not vary significantly with treatment (analysis of variance, $F(3, 16) = 2.667$, $p = 0.08$).

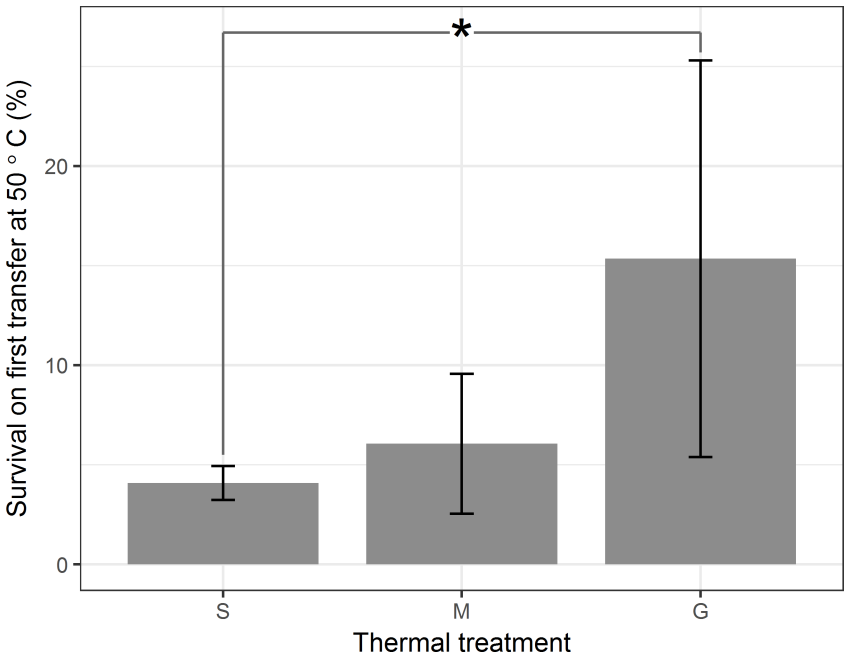

Fig 5. Average percent survival of populations on first transfer at 50˚C. Sudden populations first experienced 50˚C on Transfer 1, Moderate populations on Transfer 17, and Gradual populations on Transfer 32. Error bars represent the standard deviation of percent survival. Mean survivals are significantly different between Sudden and Gradual populations (Tukey's post-hoc test, p = 0.03).

https://doi.org/10.1371/journal.pone.0189602.g005

We reverse engineered 10 of these mutations singly into the ancestral genetic background to evaluate their effect on viral thermostability. We focused on mutations that appeared in more than one replicate (or had been previously observed in pilot experiments, S3 Table). We evaluated the effects of the single mutations on viral thermostability by exposing bacteria-free

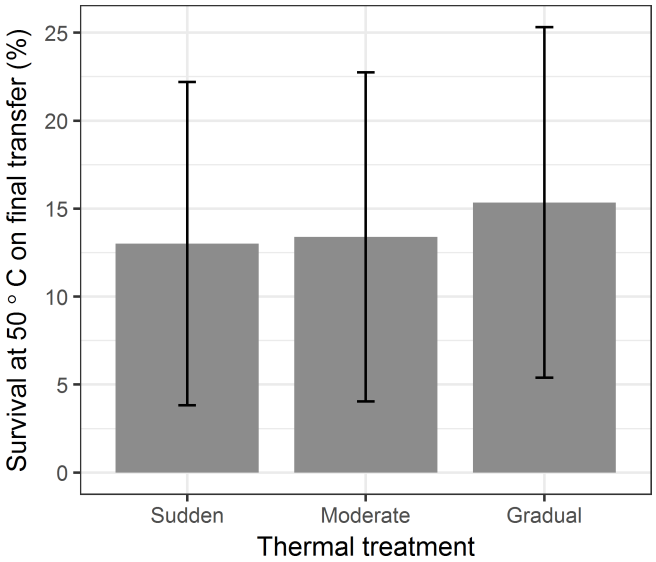

Fig 6. Average percent survival at 50˚C on the final transfer (Transfer 32) of the experiment. Error bars represent the standard deviation of percent survival. There are not significant differences in survival between treatments.

https://doi.org/10.1371/journal.pone.0189602.g006

Table 1. Mutations in genes 5 and 8 in each population at the end of the evolution experiment.

Lineage	Nucleotide change	Amino acid change
C1	*a*1989*g*	P5 R124G
C2	*a*1989*g*	P5 R124G
	*g*2282*c*	P5 *221W
C3	*a*1989*g*	P5 R124G
	*g*2276*a*	P5 W219*
C4	*a*1989*g*	P5 R124G
	*c*4259*t*	synonymous
C5	*a*1989*g*	P5 R124G
	*g*2275*a*	P5 W219*
G1	*a*510*g*	P8 Q69R
	*a*1991*t*	P5 R124S
	*g*2220*a*	P5 E201K
G2	*a*596*g*	P5 N98D
	*a*1989*g*	P5 R124G
G3	*a*1989*g*	P5 R124G
	*g*2238*t*	P5 V207F
G4	*a*510*g*	P8 Q69R
	*a*1989*g*	P5 R124G
G5	*a*596*g*	P8 N98D
	*a*1989*g*	P5 R124G
	*g*2241*a*	P5 A208T
M1	*g*629*a*	P8 V109I
	*a*1989*g*	P5 R124G
M2	*a*1675*g*	P5 K19R
	*g*2220*a*	P5 E201K
	*a*2238*a*	P5 V207I
M3	*a*1989*g*	P5 R124G
	*g*2229*c*	P5 V204L
M4	*g*629*a*	P8 V109I
	*a*1989*g*	P5 R124G
M5	*g*629*a*	P8 V109I
	*a*1989*g*	P5 R124G
S1	*a*1989*g*	P5 R124G
S2	*a*590*g*	P8 I96V
	*a*1989*g*	P5 R124G
S3	*a*590*g*	P8 I96V
	*a*1989*g*	P5 R124G
S4	*a*1989*g*	P5 R124G
S5	*a*1989*g*	P5 R124G
	*g*2220*a*	P5 E201K

Lineages are identified by their thermal treatment (C, Control; G, Gradual; M, Moderate; S, Sudden) and a replicate number (1–5). Nucleotide and amino acid changes are identified by the ancestral base (amino acid), position, and mutated base (amino acid). Nucleotide positions are numbered from the start of the NCBI Reference Sequence for the S segment of Φ6 Cystovirus (Accession# NC_003714); amino acid positions are numbered from the first amino acid of the P5 or P8 protein.

https://doi.org/10.1371/journal.pone.0189602.t001

Table 2. Number of mutations in genes encoding for P5 and P8 in each treatment.

Treatment	Number of distinct mutations in the treatment	Average number of mutations per population
Control	5	1.8
Gradual	7	2.4
Moderate	6	2.2
Sudden	3	1.6

https://doi.org/10.1371/journal.pone.0189602.t002

lysates of the mutant viruses to heat shocks ranging from 25–55˚C and measuring the lysate concentrations before and after heat shock. These data were used to build thermal kill curves, where the percent survivals at each temperature were fit to an inverse Hill equation (Eq 1) using maximum likelihood (Fig 7A).

The engineered single mutants revealed that different mutations resulted in different gains in thermostability in the ancestral background. As measured by an increase in the T_{50} parameter, six of the engineered mutations increased viral thermostability by 0.3–2.5˚C while three mutations decreased thermostability by 0.8–1.8˚C (log likelihood ratio test, $p < 0.001$; Fig 7B). In multiple cases (most evident in the Sudden treatment; see S4 Fig), populations that increased in survival had at least one thermostabilizing mutation.

Four of the six thermostabilizing mutations were conservative mutations that retained non-polar amino acids, while mutations that reduced thermostability substituted polar amino acids for ionically charged ones or vice versa. The effect size of the mutations–that is, the amount by which the mutation increased or decreased thermostability with respect to the ancestor–did not differ significantly across heat shock treatments (analysis of variance, $F(2, 25) = 0.511$, $p = 0.61$). We note, however, that the number of mutations per population was low and that not all mutations that appeared in each population were evaluated for their effects on thermostability.

Growth effects of thermostabilizing mutations

The presence of mutations that *decreased* viral thermostability suggested that these mutations may have fixed because of non-thermal selective pressures. For example, the mutation R124G in P5 appeared in 18 out of 20 different populations, including in the Control treatment, even though it reduced viral thermostability (Fig 7B). This suggested that the mutation might improve another attribute of fitness, such as viral replication. To test whether destabilizing mutations instead improved replication, we competed all engineered mutants and the ancestor against a common competitor (see section on Assaying viral competitive fitness in Methods). Many of the mutations appeared to give a competitive growth advantage in comparison to the ancestor, although some mutations decreased viral growth rates (Fig 8). All mutations that reduced thermostability seemed to increase relative competitive fitness, and many thermostabilizing mutations seemed to decrease relative competitive fitness.

A prior study in Φ6 recorded a trade-off between thermostability and growth for one mutation in P5 [41]. In our data set, several individual mutations follow the expected pattern of low T_{50} and high growth rate, or high T_{50} and low growth rate. To test for a generalized trade-off, we regressed the relative competitive fitness of the mutants against the T_{50} values estimated from the thermal kill curves (Fig 9). Although the slope of the regression line was negative, it was not statistically different from a slope of 0 (F-statistic = 0.897, df = 9, p = 0.368).

Thermostabilizing and growth effects of combinations of mutations

Several populations from heat-shocked treatments did not appear to have increased in thermostability during the evolution experiment. We expected that mutations from these populations

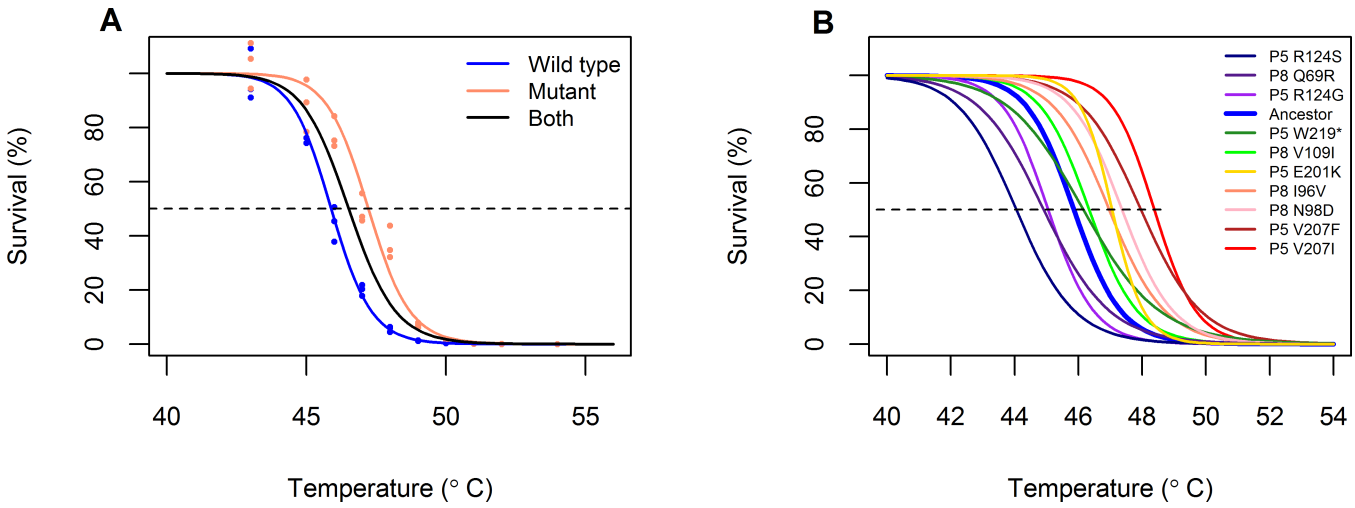

Fig 7. Thermal kill curves of engineered single mutants. A) Calculations of mutant thermostability, using the mutant P8 I96V as an example. Cell-free lysates were exposed to a 5-minute heat shock at each temperature and plated before and afterward to calculate percent survival (circles). (Note that, due to stochasticity in gauging phage titer, phage counts after heat shock can be above phage counts before heat shock, accounting for survivals greater than 100%.) Eq 1 was fitted to the data, estimating the parameters T_{50} (intersection of curve with dotted line) and n by maximum likelihood. A first model was fit to the combined data (ancestor + mutant; black curve). A second model then estimated a separate T_{50} and n for each lysate (blue, ancestor; red, mutant). The latter model was a better fit to the data (log likelihood ratio test, $p < 0.0001$). B) Empirical thermal kill curves of the ancestor (blue) and ten engineered single mutants, representing the maximum likelihood fit of all measurements taken for each mutant. Data points are omitted for simplicity. In all cases, the model that used a separate T_{50} and n for the ancestor and the mutants was a better fit to the data (log likelihood ratio test, $p < 0.001$). Pairwise comparisons with the ancestor, as in part A, can be found in the Data Repository.

https://doi.org/10.1371/journal.pone.0189602.g007

would instead have increased viral growth rates. We confirmed this hypothesis through evaluation of the thermostability and growth rates of genotypes from one of these populations (G1, replicate 1 from the Gradual treatment). Survival of the G1 population had not increased substantially over time; furthermore, it did not carry the common mutation, R124G in P5, that increased viral growth rate and was also found in Control populations (Fig 8, Table 1). From sequencing of five random plaques from Transfer 32, we found two genotypes in the final G1 population. Both genotypes shared the P5 mutation R124S (mutation B in Fig 10), but one genotype also had mutation E201K in P5 (mutation C), while the other had mutation Q69R in P8 (mutation A). As single mutations, all three increased viral growth rates, but only one (E201K) increased thermostability.

We reverse engineered these mutations in their respective double combinations (AB and BC) and evaluated their effects on thermostability and viral growth. Neither double mutant improved thermostability with respect to the ancestor (Fig 10), but both double mutants improved in relative competitive fitness with respect to the ancestor (Fig 11). Interestingly, one of the combinations exhibited sign epistasis for thermostability (mutation P8 Q69R was destabilizing in the ancestral background, but stabilizing in the P5 R124S background).

Based on historical sequencing of the G1 lineage (see S2 Text), the first mutation detected in this population (P5 R124S) decreased thermostability but enhanced viral growth. Subsequent mutations (P8 Q69R and P5 E201K) increased both thermostability and competitive fitness in the presence of P5 R124S. This sequence of mutations is consistent with stronger selection for growth rate early in a gradually changing environment and stronger selection for thermostability later on.

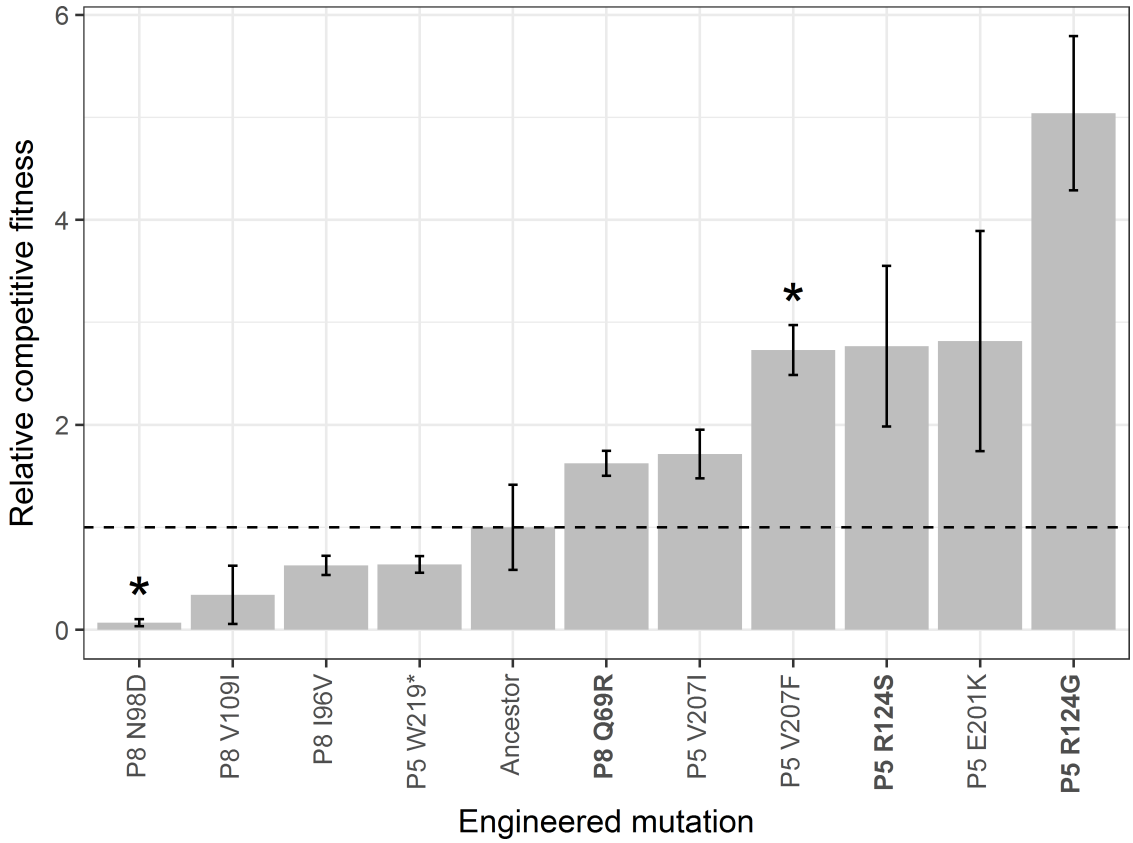

Fig 8. Competitive fitness of engineered single mutants relative to the ancestral genotype. Bar heights indicate the mean of three replicate competitions; error bars denote standard deviation. Stars denote mutants whose relative competitive fitness differs significantly from the ancestor's after a Bonferroni correction for the number of comparisons (t-test, $p < 0.001$). Mutations in bold font decrease viral thermostability relative to the ancestor.

https://doi.org/10.1371/journal.pone.0189602.g008

Discussion

The thermostability and competitive fitness of each mutation from the endpoint of our evolution experiment are summarized in Table 3. Consistent with prior work in Φ6 [42, 43], we found that virus populations exposed to high-temperature heat shocks evolved greater survival to heat shock. We also identified six causative mutations that increased viral thermostability relative to the ancestral genotype. We did not find significant differences between Gradual, Moderate, and Sudden treatments in endpoint survival at 50˚C, nor in the number, identity, or effect size of mutations. However, our conclusions are limited by the low number of replicate lineages and mutations. For example, 10 of the 16 endpoint mutations only appeared in one lineage across all treatments (Table 3), making it difficult to determine whether they arose by chance or due to selection under a particular thermal treatment. A few mutations in P8 (Q69R, N98D, V109I, and I96V) appeared in multiple times within a single treatment (Table 1, Table 3). We had previously observed these mutations in pilot lineages that were evolved with constant-temperature heat shocks (S3 Table). Specifically, Q69R and N98D from the Gradual treatment were previously observed in a pilot lineage heat shocked at 50˚C, while I96V from the Sudden treatment was observed in a pilot lineage heat shocked at 47˚C. (V109I from the Moderate treatment was also observed in a pilot lineage heat shocked at 47˚C, but Moderate lineages experienced multiple transfers both below and at 50˚C. Without knowing exactly when the mutation arose, it is unclear whether V109I was selected under particular

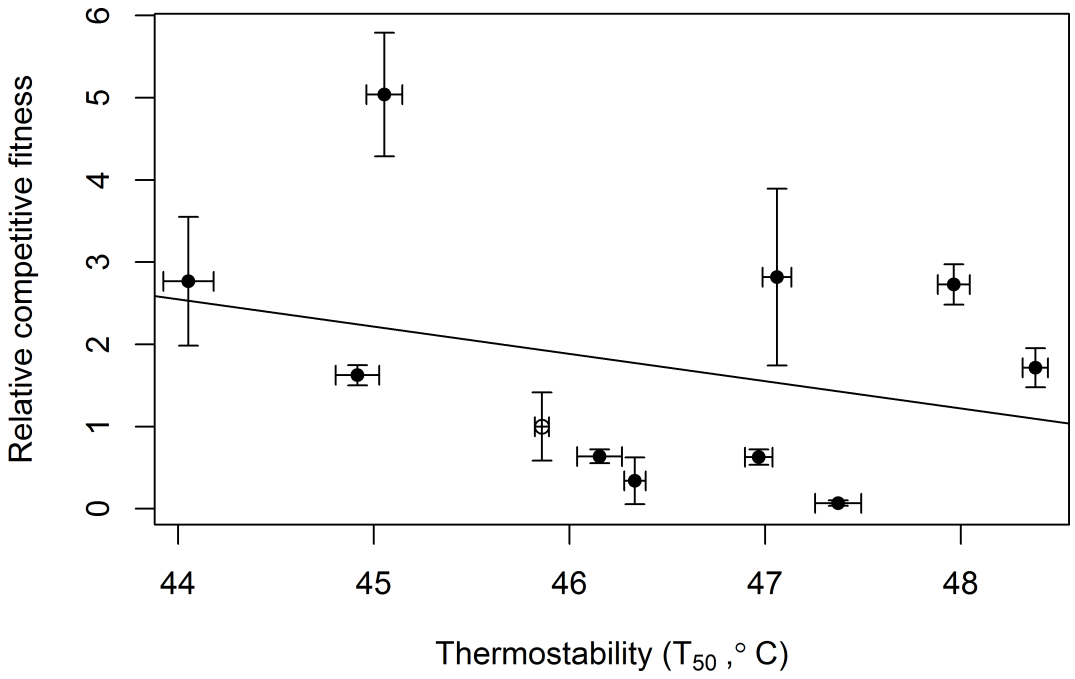

Fig 9. Relationship between relative competitive fitness and T_{50} for the ancestor and the engineered single mutants. The ancestor is marked with an open circle. X-error bars represent the standard error of the T_{50} estimate, while y-error bars represent the standard deviation of three replicate competitions. The line represents the best fit from a linear model.

https://doi.org/10.1371/journal.pone.0189602.g009

temperatures.) These mutations may be accessible for adaptation in both intermediate- and high-temperature environments, regardless of the exact rate of temperature change.

We also found that non-thermal selective pressures may have been important during the experiment. Our experimental design presented two targets for selection: on survival, under

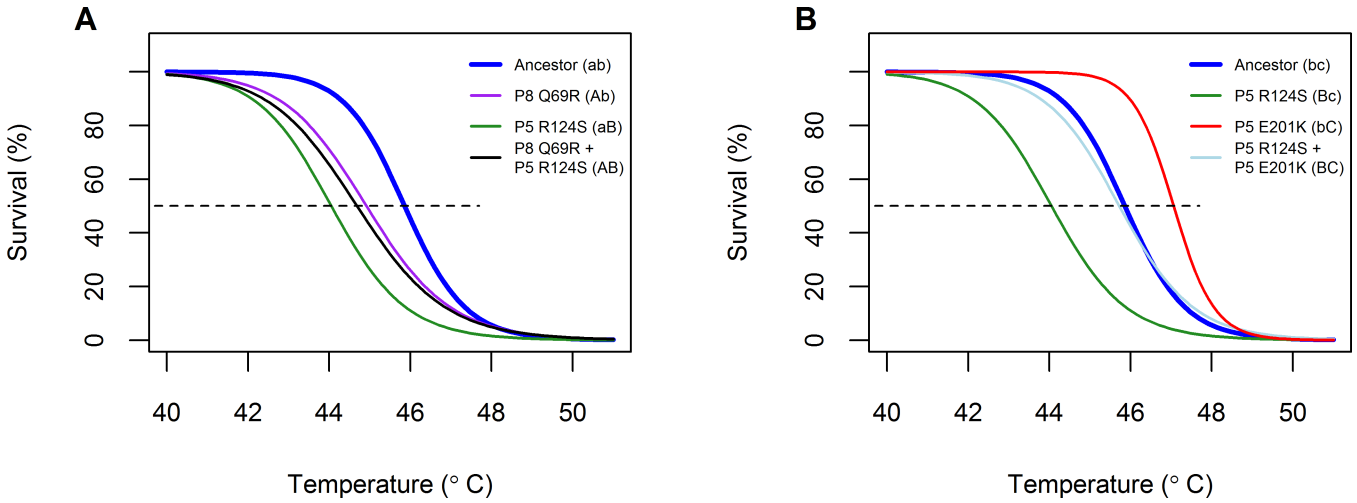

Fig 10. Evaluated thermal kill curves for two combinatorial genotypes found in one Gradual population. Mutations are given secondary labels to denote their allelic state, where a lower case letter (a, b, c) indicates the ancestral residue and an upper case letter (A, B, C) indicates the residue found in the endpoint population. A) Thermal kill curves for double mutant P8 Q69R + P5 R124S and its corresponding single mutants. B) Thermal kill curves for double mutant P5 R124S + P5 E201K and its corresponding single mutants.

https://doi.org/10.1371/journal.pone.0189602.g010

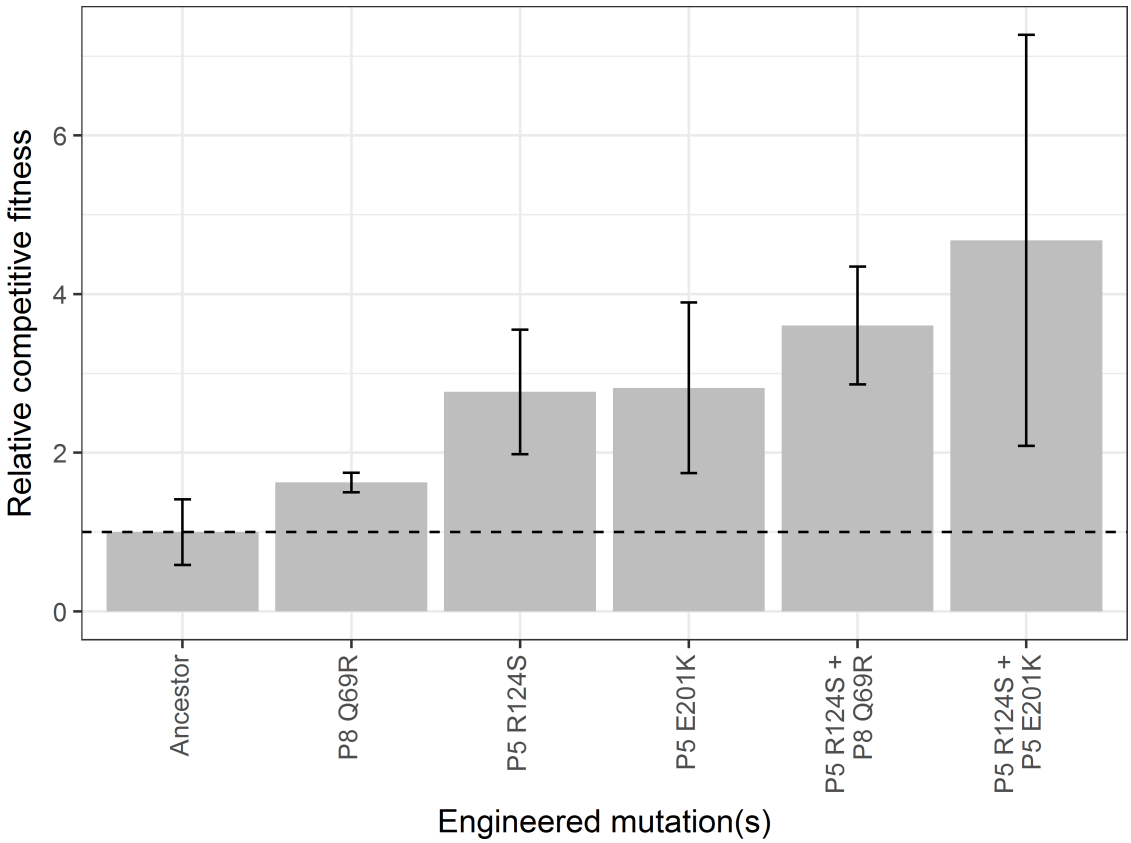

Fig 11. Relative competitive fitness of two double mutants and their constituent single mutants. Bar heights represent the mean of three replicates; error bars denote standard deviation. After a Bonferroni correction for the number of comparisons, relative competitive fitnesses of the mutants do not differ from the ancestor's. We note that addition of the double mutations did not change the overall relationship between relative competitive fitness and T_{50} shown in Fig 9.

https://doi.org/10.1371/journal.pone.0189602.g011

the high temperature heat shocks; and on replication, when viruses were grown with their bacterial host (Fig 1). Even in heat-shocked populations, we identified mutations that reduced viral thermostability but increased growth rate. The mutation that occurred most frequently across treatments, R124G in P5, enhanced growth rates rather than thermostability (Table 3), suggesting a relatively high selective pressure on viral replication, even at high temperatures. (Although we did not engineer combinations of mutations with R124G, lineages with both R124G and a thermostabilizing mutation tended to increase their survival to heat shock, while two Sudden lineages for which we found only R124G maintained low survival for the entire experiment. See also S4 Fig)

Because replication occurred at 25˚C, the typical laboratory temperature for Φ6, our experiment is reminiscent of that of Hao *et al.* [44], in which a lytic bacteriophage of *P. fluorescens* was exposed to increasing temperatures punctuated by periods of lower temperature. The authors term the fluctuations to reduced temperatures as periods of "amelioration" because they reduced selective pressures associated with heat stress. If amelioration allowed populations to recover in abundance and *de novo* mutations in the wake of an environmental stress, it could promote adaptation under stressful conditions [22, 45]. On the other hand, because amelioration relaxes the selective pressures present in a stressful environment, it may reduce the likelihood that stress-beneficial mutations will fix [46–49]. Hao *et al.* found that fewer phage populations persisted in treatments that included temperature amelioration than in

Table 3. Summary of effects of single mutations from endpoint populations on viral thermostability and competitive fitness.

Treatment	Gene	Nucleotide change	Amino acid change	Number of lineages with mutation	Thermostability (estimate, standard error)	Relative competitive fitness (mean, standard deviation)
Control	gene 5	*c*1625t	none	1	ne	ne
Control	gene 5	*a*1989*g*	R124G	5	-0.8, 0.08	5.04, 0.75
Control	gene 5	*g*2275*a*	W219*	1	ne	ne
Control	gene 5	*g*2276*a*	W219*	1	+0.3, 0.08	0.64, 0.08
Control	gene 5	g 2282*c*	*221Y	1	ne	ne
Gradual	gene 8	*a*510*g*	Q69R	2	-0.9, 0.08	1.62, 0.12
Gradual	gene 8	*a*596*g*	N98D	2	+1.5, 0.08	0.07, 0.03
Gradual	gene 5	*a*1989*g*	R124G	4	-0.8, 0.08	5.04, 0.75
Gradual	gene 5	*a*1991*t*	R124S	1	-1.8, 0.09	2.77, 0.12
Gradual	gene 5	*g*2220*a*	E201K	1	+1.2, 0.07	2.82, 1.07
Gradual	gene 5	*g*2238*a*	V207I	1	+2.5, 0.05	1.71, 0.24
Gradual	gene 5	*g*2241*a*	A208T	1	ne	ne
Moderate	gene 8	*g*629*a*	V109I	3	+0.5, 0.04	0.34, 0.28
Moderate	gene 5	*a*1675*g*	K19R	1	ne	ne
Moderate	gene 5	*a*1989*g*	R124G	4	-0.8, 0.08	5.04, 0.75
Moderate	gene 5	*g*2220*a*	E201K	1	+1.2, 0.07	2.82, 1.07
Moderate	gene 5	*g*2229*c*	V204L	1	ne	ne
Moderate	gene 5	*g*2238*t*	V207F	1	+2.1, 0.06	2.73, 0.24
Sudden	gene 8	*a*590*g*	I96V	2	+1.1, 0.06	0.63, 0.09
Sudden	gene 5	*a*1989*g*	R124G	5	-0.8, 0.08	5.04, 0.75
Sudden	gene 5	*g*2220*a*	E201K	1	+1.2, 0.07	2.82, 1.07

Nucleotide and amino acid changes are identified by the ancestral base (amino acid), position, and mutated base (amino acid). Nucleotide positions are numbered from the start of the NCBI Reference Sequence for the S segment of Φ6 Cystovirus (Accession# NC_003714); amino acid positions are numbered from the first amino acid of the P5 or P8 protein. Thermostability is given as the T_{50} estimate and standard error of the estimate from the maximum likelihood model of viral thermal kill curves. Relative competitive fitness is given as the mean and standard deviation from three replicate competitions. Mutations that were not evaluated in this study are marked with "ne."

https://doi.org/10.1371/journal.pone.0189602.t003

treatments where the temperature increased monotonically, indicating that periods of amelioration hindered adaptation at high temperatures. Although we did observe increases in

thermostability over the course of our evolution experiment, we cannot rule out the possibility that thermostability evolution was hindered due to periods of growth at 25˚C.

Amelioration is especially likely to impede adaptation to stressful environments if stress-beneficial mutations impose fitness costs under more benign conditions [44]. A prior study in Φ6 found that a highly thermostabilizing mutation decreased the ability of viruses to replicate at 25˚C [41]. We did not find support for a general trade-off between thermostability and rates of viral replication in our data (Fig 9). However, we can identify mutations in P5 and P8 that showed a pattern of either high thermostability but low growth rates, or low thermostability but high growth rates. Interestingly, some mutations appeared to increase both thermostability and growth rate. (We note that this last class includes V207F in P5, which has previously been reported to increase thermostability but *decrease* viral growth rates [41]. We speculate that this is because the genetic background of our phage differed from the genotype used in [41].) It is possible that our sample of 11 genotypes is too limited to permit detection of a general trade-off. Alternatively, mutations that contribute to thermostability may not always be constrained by trade-offs. For example, due to their high mutation rates, viruses can find "cost free" adaptations [50–52], which allow them to maintain existing functions while gaining new ones. Such mutations may be particularly important during evolution in changing environments. It is also possible that we did not sample mutations that demonstrate a trade-off, since we examined mutations found at the end of the experiment. Mutations that may have exhibited a trade-off between thermostability and growth rates and were present at earlier time points might have been outcompeted by mutations that performed well in both dimensions.

That we find growth-enhancing but thermo-destabilizing mutations, however, highlights that organisms experience selective pressures along multiple phenotypic axes. This has potential implications for evolution in environments that change incrementally. For example, a gradually changing thermal environment imposes small differences in selective pressure on the population from generation to generation. In this case, the population may experience stronger relative selective pressure along a non-thermal axis, such as for growth. The population may then not evolve in response to the thermal environment until sufficient thermal change has occurred and relative selective pressures are high enough. Gorter *et al.* [26] report that, in a yeast system, adaptation to general culture conditions preceded adaptation to high metal concentrations under conditions where the metal concentration increased slowly. Similarly, we note that while the first detectable mutation in one Gradual lineage reduced viral thermostability but enhanced growth, both mutations that rose to prominence later in the evolution of this lineage were thermostabilizing in the background of the first mutation (see S2 Text for historical sequencing of this lineage).

In extreme cases, evolution in response to a non-focal selective pressure may impose trade-offs or constraints in the changing stressful environment. Suppose, for example, that evolution for higher growth rates always reduced thermostability. Populations that experienced a gradual increase in temperature may have first fixed growth-enhancing mutations because of stronger relative selective pressures for growth than for thermostability. However, these mutations would have lowered the thermostability of the population, even as thermal stress became a more prominent selective pressure over time. The population would then be in a *worse* place, in terms of thermostability, than when it started, and mutations of larger thermostabilizing effect would be required to increase its survival at high temperatures. Although we are unaware of any empirical studies that look explicitly at the role of such trade-offs in incrementally changing environments, this conclusion is in the spirit of studies that predict greater phenotypic and genotypic constraint under slow environmental change (e.g., [7, 15, 18, 53]).

Other results from this study are consistent with prior work on adaptation under varying rates of environmental change.

Evidence from prior experiments (e.g., [20–23]) suggests that evolution in a mildly stressful environment (such as an intermediate temperature) can enhance a population's ability to withstand a more stressful environment (such as a high temperature). Consistent with this expectation, populations from the Gradual treatment had a higher average survival on their first exposure to 50˚C than did populations from the Sudden treatment on their first exposure. In other words, exposure to intermediate temperatures can promote survival of Φ6 at high temperatures.

Several prior experiments found a greater diversity of mutations under rapid than gradual environmental change [7, 19, 25]. In contrast, we find a (non-significant) pattern of more mutations in endpoint Gradual and Moderate populations compared to Sudden populations. This could represent a greater amount of clonal interference in Gradual and Moderate than Sudden lineages (e.g., [24, 28]). (Consider, for example, that lineage G1 had two high-frequency genotypes at the endpoint of the experiment. Sequencing the lineage at prior time points [see S2 Text] furthermore suggested that both these genotypes were still increasing in frequency when the experiment ended.)

Another possibility is that mutations that increase thermostability do not vary with thermal treatment. A study that examined the thermal adaptation of the bacteriophage Qβ found that populations evolved under a constant high temperature did not significantly differ in evolutionary outcomes from populations evolved under fluctuating temperatures [54]. In this study, when we include data from pilot experiments, most of the engineered mutations appeared in populations that had experienced diverse heat shock treatments (S3 Table). Proteins tend to be marginally stable and can be destabilized by single amino acid substitutions [55–57], including mutations that are adaptive for functions besides stability (e.g., ligand binding [58, 59] or growth [60]). In contrast, computational and empirical data sets suggest that relatively few substitutions will increase a protein's thermostability [56, 57, 61]. In the case of an enzyme, such as the P5 lysis protein in Φ6, any mutations that increase stability must simultaneously maintain the flexibility or activity necessary for the protein's function [55]. Notably, we found 5 mutations across heat-shocked treatments in amino acid positions 201–208 of P5. Three mutations (E201K, V207F, and V207I) increased viral thermostability. (We were not able to engineer the other two mutations, V204L and A208T, but their corresponding lineages increased in survival during the evolution experiment.) In the P5 protein, all of these mutations are physically close to V207F, which has previously been shown to increase thermostability by filling an empty hydrophobic pocket [41]. The number of mutations that increase thermostability may thus be small and/or biochemically constrained for particular proteins, resulting in relatively few mutational pathways for improvement.

It is also possible that the stringent bottlenecks we imposed on our experimental lineages muted differences in the number of mutations in each treatment. Because of lower selective pressures, population sizes tend to be larger in environments that change gradually than rapidly, which may contribute to greater genetic diversity [21, 24]. Our small bottlenecks may have stochastically removed low-frequency mutations, reducing the diversity of our populations [62, 63]. On the other hand, the stringent bottlenecks may have contributed to the fixation of mutations that increased viral replication rates over thermostability by increasing relative selective pressures for growth during the evolution experiment.

Overall, our study emphasizes that it is important to take *all* selective pressures into account during an evolution experiment. We found that populations that did not increase in thermostability appeared to have evolved higher replication rates. We speculate that this may offer an alternative way for populations to persist under heat shock, rather than improving their thermostability: They may be able to compensate for reductions in population size due to heat shock by subsequently replicating more rapidly. This highlights the conclusion that multiple

features of organisms can evolve, even in environments that change in only a single focal factor.

Supporting information

S1 Table. Strains used and engineered in this study. Laboratory collection numbers (BK numbers) are included for request purposes. All other data presented in this study (including this table, other Supporting Information, and the Data Repository) use the project-specific (PRESS) numbers. Mutations are labeled in order ancestral base (amino acid)—position—mutated base (amino acid), where the position is measured from the first nucleotide of the NCBI Reference Sequence for the S segment of Φ6 Cystovirus (Accession# NC_003714) or the first amino acid of the protein. We also note the presence of any additional (i.e., non-engineered) mutations present in the mutant viral clones. We account for the effects of these mutations with the "matched" viral clones; see S1 Text.
(XLSX)

S2 Table. Heat shock temperatures used at each transfer in the experimental treatments.
(XLSX)

S3 Table. Mutations from the evolution experiment found in pilot experiments. During pilot experiments, replicate lineages of the ancestral Φ6 used in this study were propagated for 30 transfers with heat shocks at a constant temperature between 45˚C and 52˚C. In these lineages, the heat shock temperature is denoted by "T" (e.g., "T47" indicates the lineage was heat shocked at 47˚C), and "R" indicates the replicate number assigned to the population (e.g., "R1" indicates replicate 1). Mutations found in multiple replicate populations, e.g. populations 1, 2, and 3, are denoted with dashes, e.g., R1-3. Lineages from the evolution experiment presented in this study are denoted with a letter representing their treatment (Gradual, G; Moderate, M; Sudden, S; and Control, C) and a number indicating the replicate. Nucleotide changes are numbered from the start of the NCBI Reference Sequence for the S segment of Φ6 Cystovirus (Accession# NC_003714); amino acid changes are numbered from the first amino acid of the protein.
(XLSX)

S4 Table. Primers used for reverse engineering of Φ6 mutants. The engineered mutation is indicated with upper case in the nucleotide sequence. Where not otherwise stated in Reverse engineering (Methods), primers were prepared according to instructions in the QuikChange II mutagenesis kit. Primers for mutant V109I in P8 were given a standard desalting and used in a T4 ligation reaction; melting temperatures for these primers were calculated using the OligoAnalyzer (Integrated DNA Technologies, https://www.idtdna.com/calc/analyzer).
(XLSX)

S1 Fig. Measured survival of the ancestral genotype at 25˚C. The survival of three replicates was measured on six different days. On five of the days, measured baseline survival of the ancestor at its typical growth temperature was greater than 100%.
(TIF)

S2 Fig. Comparison of ancestral thermal kill curves with and without asymptote adjustment. Temperatures from 42–51˚C are shown to highlight the region where survival decreased the most. Survivals were taken across the range of heat shock temperatures on six different days. Eq 1 was fit to each day separately. The unadjusted model (black lines) used the survival data as measured (black circles), fixing the asymptote (parameter *a*) at 100%. For the asymptote-adjusted model, parameter *a* was allowed to vary across days. Survival values were then

divided by their respective asymptote (blue triangles; offset horizontally for better visualization), and Eq 1 re-fit to the adjusted data (blue lines). T_{50} values (intersection of the curves with the dotted line) were more similar across days when the data were not adjusted for varying asymptotes.
(TIF)

S3 Fig. Competitive fitness of the ancestral genotype initialized at different frequencies. Competitions were initialized with target starting ratios of ancestor: common competitor at 1: 5, 1: 10, 1: 50, and 1: 100. (An initial ratio of 1: 1 yielded a final concentration of common competitor that was too low for reliable fitness estimates.) Competitive fitness was calculated using Eq 2. The mean competitive fitness is indicated with a dashed line. The competitive fitness values of the ancestral genotype are not significantly correlated with its initial frequency (Pearson's correlation test, ρ = -0.32, p = 0.30).
(TIF)

S4 Fig. Changes in percent survival of Sudden populations with and without thermostabilizing mutations. At each transfer, the survival of each population (Observed percent survival) was compared to the percent survival of the ancestor (Expected percent survival) at 50˚C. Lineages are distinguished according to whether at least one thermostabilizing mutation was present in the endpoint population. (Note that, although the entire lineage has been colored for the purpose of visualization, the exact point in time at which the thermostabilizing mutation arose was not evaluated in this study.)
(TIF)

S1 Text. Effects of additional mutations in the engineered viral mutants on thermostability and relative competitive fitness.
(PDF)

S2 Text. Historical sequencing of population Gradual 1.
(PDF)

Acknowledgments

We thank E. Cooper, C. Dunnell, E. Hsieh, and K. van Raay for their assistance in troubleshooting and collecting data for this study; and P.L. Conlin and H. Jordt for comments on the manuscript.

Author Contributions

Conceptualization: Sonia Singhal, Benjamin Kerr.

Data curation: Sonia Singhal, Cierra M. Leon Guerrero.

Formal analysis: Sonia Singhal.

Funding acquisition: Sonia Singhal, Cierra M. Leon Guerrero, Erin M. McClure, Benjamin Kerr.

Investigation: Sonia Singhal, Cierra M. Leon Guerrero, Stella G. Whang, Erin M. McClure, Hannah G. Busch.

Methodology: Sonia Singhal, Cierra M. Leon Guerrero, Stella G. Whang, Erin M. McClure, Hannah G. Busch.

Project administration: Sonia Singhal.

Resources: Benjamin Kerr.

Software: Sonia Singhal.

Supervision: Sonia Singhal.

Validation: Sonia Singhal, Cierra M. Leon Guerrero, Stella G. Whang, Erin M. McClure, Hannah G. Busch.

Visualization: Sonia Singhal, Benjamin Kerr.

Writing – original draft: Sonia Singhal, Cierra M. Leon Guerrero, Stella G. Whang, Erin M. McClure, Hannah G. Busch.

Writing – review & editing: Sonia Singhal, Cierra M. Leon Guerrero, Stella G. Whang, Erin M. McClure, Hannah G. Busch, Benjamin Kerr.

References

1. Orr HA. The population genetics of adaptation: The distribution of factors fixed during adaptive evolution. Evolution 1998; 52:935–49. https://doi.org/10.1111/j.1558-5646.1998.tb01823.x PMID: 28565213
2. Fisher R.A. The genetical theory of natural selection. New York: Dover; 1958.
3. Davis MB, Shaw RG. Range shifts and adaptive responses to quaternary climate change. Science 2001; 292:673–9. https://doi.org/10.1126/science.292.5517.673 PMID: 11326089
4. Keeling CD, Whorf TP, Wahlen M, van der Plicht J. Interannual extremes in the rate of rise of atmospheric carbon dioxide since 1980. Nature 1995; 375:666–70.
5. Warneke C, de Gouw JA, Holloway JS, Peischl J, Ryerson TB, Atlas E, et al. Multiyear trends in volatile organic compounds in Los Angeles, California: Five decades of decreasing emissions. J. Geophys. Res. 2012; 117:D00V17.
6. Bello Y, Waxman D. Near-periodic substitution and the genetic variance induced by environmental change. J. Theor. Biol. 2009; 239:152–60.
7. Collins S, de Meaux J, Acquisti C. Adaptive walks toward a moving optimum. Genetics 2007; 176:1089–99. https://doi.org/10.1534/genetics.107.072926 PMID: 17435242
8. Kopp M, Hermisson J. Adaptation of a quantitative trait to a moving optimum. Genetics 2007; 176:715–9. https://doi.org/10.1534/genetics.106.067215 PMID: 17409085
9. Lynch M, Gabriel W, Wood AM. Adaptive and demographic responses of plankton populations to environmental change. Limnol. Oceanogr. 1991; 36:1301–12.
10. Lynch M, Lande R. Evolution and extinction in response to environmental change. In: Kareiva PM, Kingsolver JG, Huey RB, editors. Biotic interactions and global change. Sunderland, Massachusetts: Sinauer; 1993. p. 234–50.
11. Bürger R, Lynch M. Evolution and extinction in a changing environment: A quantitative-genetic analysis. Evolution 1995; 49:151–63. https://doi.org/10.1111/j.1558-5646.1995.tb05967.x PMID: 28593664
12. Gomulkiewicz R, Houle D. Demographic and genetic constraints on evolution. Am. Nat. 2009; 174(6): E218–29. https://doi.org/10.1086/645086 PMID: 19821744
13. Kopp M, Matuszewski S. Rapid evolution of quantitative traits: theoretical perspectives. Evol. Appl. 2014; 7:169–91. https://doi.org/10.1111/eva.12127 PMID: 24454555
14. Pease CM, Lande R, Bull JJ. A model of population growth, dispersal and evolution in a changing environment. Ecology 1989; 70(6):1657–64.
15. Broom M, Tang Q, Waxman D. Mathematical analysis of a model describing evolution of an asexual population in a changing environment. Math. Biosci. 2003; 186:93–108. PMID: 14527749
16. Chevin L-M. Genetic constraints on adaptation to a changing environment. Evolution 2013; 67:708–21. https://doi.org/10.1111/j.1558-5646.2012.01809.x PMID: 23461322
17. Gomulkiewicz R, Holt RD. When does evolution by natural selection prevent extinction? Evolution 1995; 49(1):201–7. https://doi.org/10.1111/j.1558-5646.1995.tb05971.x PMID: 28593677
18. Bell G, Collins S. Adaptation, extinction and global change. Evol. Appl. 2008; 1:3–16. https://doi.org/10.1111/j.1752-4571.2007.00011.x PMID: 25567487

19. Perron GG, Gonzalez A, Buckling A. The rate of environmental change drives adaptation to an antibiotic sink. J. Evol. Biol. 2008; 21:1724–31. https://doi.org/10.1111/j.1420-9101.2008.01596.x PMID: 18681913

20. Bell G, Gonzalez A. Adaptation and evolutionary rescue in metapopulations experiencing environmental deterioration. Science 2011; 332:1327–30. https://doi.org/10.1126/science.1203105 PMID: 21659606

21. Lindsey H, Gallie J, Taylor S, Kerr B. Evolutionary rescue from extinction is contingent on a lower rate of environmental change. Nature 2013; 494:463–6. https://doi.org/10.1038/nature11879 PMID: 23395960

22. Samani P, Bell G. Adaptation of experimental yeast populations to stressful conditions in relation to population size. J. Evol. Biol. 2010; 23:791–6. https://doi.org/10.1111/j.1420-9101.2010.01945.x PMID: 20149025

23. Baym M, Lieberman TD, Kelsic ED, Chait R, Gross R, Yelin I, et al. Spatiotemporal microbial evolution on antibiotic landscapes. Science 2016; 353:1147–51. https://doi.org/10.1126/science.aag0822 PMID: 27609891

24. Collins S, de Meaux J. Adaptation to different rates of environmental change in Chlamydomonas. Evolution 2008; 63:2952–65.

25. Morley VJ, Mendiola SY, Turner PE. Rate of novel host invasion affects adaptability of evolving RNA virus lineages. Proc. R. Soc. B 2015; 282:20150801. https://doi.org/10.1098/rspb.2015.0801 PMID: 26246544

26. Gorter FA, Aarts MMG, Zwaan BJ, de Visser JAGM. Dynamics of adaptation in experimental yeast populations exposed to gradual and abrupt change in heavy metal concentration. Am. Nat. 2016; 187:110–9. https://doi.org/10.1086/684104 PMID: 27277407

27. Gerrish PJ, Lenski RE. The fate of competing beneficial mutations in an asexual population. Genetica 1998; 102/103:127–44.

28. Morley VJ, Turner PE. Dynamics of molecular evolution in RNA virus populations depend on sudden versus gradual environmental change. Evolution 2017; 71:872–83. https://doi.org/10.1111/evo.13193 PMID: 28121018

29. Mindich L, MacKenzie G, Strassman J, McGraw T, Metzger S, Romantschuk M, et al. cDNA cloning of portions of the bacteriophage phi-6 genome. J. Bacteriol. 1985; 162:992–9. PMID: 3858275

30. Mindich L. Reverse genetics of dsRNA bacteriophage phi-6. Adv. Vir. Res. 1999; 53:341–53.

31. Mindich L, Qiao X, Onodera S, Gottlieb P, Frilander M. RNA structural requirements for stability and minus-strand synthesis in the dsRNA bacteriophage Φ6. Virology 1994; 202:258–63. https://doi.org/10.1006/viro.1994.1341 PMID: 8009837

32. Onodera S, Olkkonen VM, Gottlieb P, Strassman J, Qiao X, Bamford DH, et al. Construction of a transducing virus from double-stranded RNA bacteriophage phi6: Establishment of carrier states in host cells. J. Virol. 1992; 66:190–6. PMID: 1727482

33. Frilander M, Gottlieb P, Strassman J, Bamford DH, Mindich L. Dependence of minus-strand synthesis on complete genomic packaging in the double-stranded RNA bacteriophage ϕ6. J. Virol. 1992; 66:5013–7. PMID: 1629962

34. Gottlieb P, Strassman J, Qiao X, Frilander M, Frucht A, Mindich L. In vitro packaging and replication of individual genomic segments of bacteriophage ϕ6 RNA. J. Virol. 1992; 66:2611–16. PMID: 1560520

35. Onodera S, Qiao X, Gottlieb P, Strassman J, Frilander M, Mindich L. RNA structure and heterologous recombination in the double-stranded RNA bacteriophage Φ6. J Virol. 1993; 67(8):4914–22. PMID: 8331732

36. Davanloo P, Rosenberg AH, Dunn JJ, Studier FW. Cloning and expression of the gene for bacteriophage T7 RNA polymerase. PNAS 1984; 81:2035–39. PMID: 6371808

37. Sun Y, Qiao X, Mindich L. Construction of carrier stat viruses with partial genomes of the segmented dsRNA bacteriophages. Virology 2004; 319:274–9. https://doi.org/10.1016/j.virol.2003.10.022 PMID: 14980487

38. Hanahan D. Studies on transformation of Escherichia coli with plasmids. J. Mol. Biol. 1983; 166:557–80. PMID: 6345791

39. Mindich L, Lehman J. Cell wall lysin as a component of the bacteriophage ϕ6 virion." J. Virol. 1979; 30:489–96. PMID: 469991

40. Olkkonen VM, Ojala P, Bamford DH. Generation of infectious nucleocapsids by in vitro assembly of the shell protein onto the polymerase complex of the dsRNA bacteriophage ϕ6. J. Mol. Biol. 1991; 218:569–81. PMID: 2016747

41. Dessau M, Goldhill D, McBride RL, Turner PE, Modis Y. Selective pressure causes an RNA virus to trade reproductive fitness for increased structural and thermal stability of a viral enzyme. PLOS Genet. 2012; 8:e1003102. https://doi.org/10.1371/journal.pgen.1003102 PMID: 23209446

42. McBride RC, Ogbunugafor CB, Turner PE. Robustness promotes evolvability of thermotolerance in an RNA virus. BMC Evol. Biol. 2008; 8:231–45. https://doi.org/10.1186/1471-2148-8-231 PMID: 18694497

43. Goldhill D, Lee A, Williams ESCP, Turner PE. Evolvability and robustness in populations of RNA virus ϕ6. Front. Microbiol. 2014; 5:35. https://doi.org/10.3389/fmicb.2014.00035 PMID: 24550904

44. Hao Y-Q, Brockhurst MA, Petchey OL, Zhang Q-G. Evolutionary rescue can be impeded by temporary environmental amelioration. Ecol. Lett. 2015; 18:892–8. https://doi.org/10.1111/ele.12465 PMID: 26119065

45. Wahl LM, Gerrish PJ, Saika-Vovoid I. Evaluating the impact of population bottlenecks in experimental evolution. Genetics 2002; 162:961–71. PMID: 12399403

46. Uecker H, Hermisson J. On the fixation process of a beneficial mutation in a variable environment. Genetics 2011; 188:915–30. https://doi.org/10.1534/genetics.110.124297 PMID: 21652524

47. Peischl S, Kirkpatrick M. Establishment of new mutations in changing envionments. Genetics 2012; 191:895–906. https://doi.org/10.1534/genetics.112.140756 PMID: 22542964

48. Kirkpatrick M, Peischl S. Evolutionary rescue by beneficial mutations in environments that change in space and time. Philos. Trans. R. Soc. B 2013; 368:20120082.

49. Alto BW, Wasik BR, Morales NM, Turner PE. Stochastic temperatures impede RNA virus adaptation. Evolution 2013; 67:969–79. https://doi.org/10.1111/evo.12034 PMID: 23550749

50. Duffy S, Turner PE, Burch CL. Pleiotropic costs of niche expansion in the RNA bacteriophage Φ6. Genetics 2006; 172:751–7. https://doi.org/10.1534/genetics.105.051136 PMID: 16299384

51. Ford BE, Sun B, Carpino J, Chapler ES, Ching J, Choi Y, et al. Frequency and fitness consequences of bacteriophage Φ6 host range mutants. PLOS ONE 2014; 9:e113078. https://doi.org/10.1371/journal.pone.0113078 PMID: 25409341

52. Turner PE, Morales NM, Alto BW, Remold SK. Role of evolved host breadth in the initial emergence of an RNA virus. Evolution 2010; 64:3273–86. https://doi.org/10.1111/j.1558-5646.2010.01051.x PMID: 20633045

53. Waxman D, Peck JR. Sex and adaptation in a changing environment. Genetics 1999; 153:1041–53. PMID: 10511577

54. Arribas M, Kubota K, Cabanillas L, Lázaro E. Adaptation to fluctuating temperatures in an RNA virus is driven by the most stringent selective pressure. PLOS ONE 2014; 9:e100940. https://doi.org/10.1371/journal.pone.0100940 PMID: 24963780

55. Somero GN. Proteins and temperature. Annu. Rev. Physiol. 1995; 57:43–68. https://doi.org/10.1146/annurev.ph.57.030195.000355 PMID: 7778874

56. Tokuriki N, Stricher F, Schymkowitz J, Serrano L, Tawfik DS. The stability effects of protein mutations appear to be universally distributed. J. Mol. Biol. 2007; 369:1318–22. https://doi.org/10.1016/j.jmb.2007.03.069 PMID: 17482644

57. Tokuriki N, Tawfik DS. Stability effects of mutations and protein evolvability. Curr. Opin. Struct. Biol. 2009; 19:596–604. https://doi.org/10.1016/j.sbi.2009.08.003 PMID: 19765975

58. Bloom JD, Silberg JJ, Wilke CO, Drummond DA, Adami C, Arnold FH. Thermodynamic prediction of protein neutrality. PNAS 2005; 102:606–11. https://doi.org/10.1073/pnas.0406744102 PMID: 15644440

59. Bloom JD, Labthavikul ST, Otey CR, Arnold FH. Protein stability promotes evolvability. PNAS 2006; 103:5869–74. https://doi.org/10.1073/pnas.0510098103 PMID: 16581913

60. Gong LI, Suchard MA, Bloom JD. Stability-mediated epistasis constrains the evolution of an influenza protein. eLife 2013; 2:e00631. https://doi.org/10.7554/eLife.00631 PMID: 23682315

61. Tokuriki N, Stricher F, Serrano L, Tawfik DS. How protein stability and new functions trade off. PLOS Comp. Biol. 2008; 4:e1000002.

62. Wahl LM, Gerrish PJ, Saika-Voivoid I. Evaluating the impact of population bottlenecks in experimental evolution. Genetics 2002; 162:961–71. PMID: 12399403

63. Vogwill T, Phillips RL, Gifford DR, MacLean CR. Divergent evolution peaks under intermediate population bottlenecks during bacterial experimental evolution. Proc. R. Soc. B 2016; 283:20160749. https://doi.org/10.1098/rspb.2016.0749 PMID: 27466449